# Effect of parcel models on particles' dispersion and gas-particle two-phase interaction in a particle-laden turbulent mixing layer

Masaya MUTO*, Hiroaki WATANABE
Central Research Institute of Electric Power Industry, Japan
masayam@criepi.denken.or.jp and whiroaki@criepi.denken.or.jp

**Abstract**

A three-dimensional DNS is performed in a particle-laden turbulent mixing layer to investigate effects of a parcel modeling on particles spatial dispersion, exchange of momentum, and interphase mass transfer which is represented by nonreactive scalar distribution evaporated from dispersed particles. Two parcel models in which each parcel has the same volume (volume fixed model, VFM) and represents the same number of particles (number fixed model, NFM) are discussed by comparing with directly tracking one by one particle without parcel model as a referred case (reference case, RC). Results show that difference in the characteristics of particle dispersion is observed between VFM and RC, while good agreement is found between NFM and RC at the upstream region of the mixing layer. However, it is found in comparing with RC that an underestimation of momentum transfer appears for VFM and NFM in whole region of the mixing layer. This is because the parcels exchange a large amount of momentum in the limited small spaces and the relative velocity is decreased locally, and then the momentum exchange is suppressed. Parcel models also cause an underestimation of evaporation from particles compared to RC. Especially, VFM is more likely to underestimate the total amount of evaporation compared to NFM.

## Introduction

Particle-laden turbulent flows are encountered in a number of engineering applications such as energy conversion and internal combustion devices using solid or liquid fuel. Therefore it is highly important to understand the effects of laden particles on turbulence and the dispersivity of particles in turbulent flow fields. In most practical particle-laden turbulent flows, the particle mass fraction often becomes large owing to a large density ratio of solid or liquid particle to ambient gas, hence the modulation of flow field by particles should be considered. Recently, there are several studies were performed for inhomogeneous turbulent flows such as a spatially developed mixing layer and a jet, in which the physical mechanisms of turbulent modulation may change with the streamwise distance. As previous fundamental studies, Yang *et al*. (1990)[1] and Dimas and Kiger (1998)[2] investigated the stability of two-way coupled mixing layers with uniformly distributed particles by linear stability analysis and Michioka *et al*. (2005)[3] investigated the effects of laden particles on turbulence, chemical species diffusion and reaction using mixing layer. In such predictions of scalar distribution, diffusion of the scalar is affected by not only the modulated flow field due to the particles but also dispersed particles because of its evaporavility depending on particle spatial density. In the traditional approach for particle-laden flow computation, the Eulerian equations for gaseous phase are solved along with a Lagrangean model for particle transport[4, 5]. However, tracing every particle in Lagrangean manner is difficult for practical purpose because the number of particles in most engineering applications is huge. Therefore a parcel model is generally employed in the Eulerian-Lagrangean numerical procedures to reduce computational cost.

In the parcel model, a certain number of particles are represented by one parcel and the parcels are traced in flow field instead of each particle. Here we can consider two types of parcel model. The first model is that each parcel has the same volume (volume fixed model, VFM), which is generally used in commercial software on gas-particle two-phase flow. In this model the smaller particle diameter becomes, the larger the number of particles is represented by one parcel. Another model is that each parcel represents the same number of particles (number fixed model, NFM). In this model the smaller the particle diameter becomes, the larger the number of parcels increases. Both models have been used in existing studies but few reports on a difference between two models exist in spite of that the probability density function of the number of parcels is significantly different between two models. Furthermore, recently, it was reported that the use of parcel approach has a risk of causing a prediction error in spray combustion. This is because the parcels release a large amount of fuel vapor in the limited small spaces. This increases the partial fuel vapor pressure at limited locations, and suppresses the global droplet evaporation rate[6]. However, an effective number of particles that each parcel represents on the change of flow field compared to the case of without parcel model case is not reported so far.

*Corresponding author: masayam@criepi.denken.or.jp

So in this study, effects of parcel models on particles' dispersion, two-phase momentum interaction and interphase mass transfer which is represented by nonreactive scalar distribution evaporated from dispersed particles are investigated using direct numerical simulation (DNS) in turbulent mixing layer. In this study, One parcel represents about 10 particles when VFM is applied and exactly 10 particles when NFM is applied. To validate both models, a base case in which parcel model is not applied (reference case, RC) is also implemented as a reference.

**Numerical and/or Experimental Methods**

***Government equations and discretization***

The governing equations for particle-laden turbulent flow with evaporation are continuity, momentum (Navier-Stokes), energy and mass conservation equations described as equations (1) to (4) and are discretized by using the vertex-centered finite volume method. Second-order central differences approximations are used to discretize the spatial derivative, while 5% of the first order upwind scheme is blended with the central differences to estimate the convective flux on the cell surface. The time marching is based on the fractional step method in which the first-order Euler implicit scheme is used for velocity prediction. The coupling of the velocity and pressure fields is based on the simplified marker and cell (SMAC) method.

$$\frac{\partial \rho}{\partial t} + \frac{\partial}{\partial x_j}\left(\rho u_j\right) = S_m, \tag{1}$$

$$\frac{\partial \rho u_i}{\partial t} + \frac{\partial}{\partial x_j}\left(\rho u_i u_j\right) + \frac{\partial P}{\partial x_j} - \frac{\partial}{\partial x_j}\left(\mu \frac{\partial u_i}{\partial x_j}\right) = S_{ui}, \tag{2}$$

$$\frac{\partial \rho h}{\partial t} + \frac{\partial}{\partial x_j}\left(\rho u_j h \rho a \frac{\partial h}{\partial x_j} + \sum_{k=1}^{n} h_k(\rho a - \rho D_k)\frac{\partial Y_k}{\partial x_j}\right) = S_h, \tag{3}$$

$$\frac{\partial \rho Y_k}{\partial t} + \frac{\partial}{\partial x_j}\left(\rho u_j Y_k - \rho D_k \frac{\partial Y_k}{\partial x_j}\right) = S_{Y_k}, \tag{4}$$

where $u_i$ is the gaseous phase velocity, $\rho$ is the density, $\mu$ is the viscosity, $P$ is the static pressure, $h$ is the specific total enthalpy, $a$ is the gaseous thermal diffusivity, and $h_k$, $Y_k$, and $D_k$ are the specific enthalpy, the scalar fraction, and the scalar diffusion coefficient of the $k$th species, respectively. The gaseous phase density, $\rho$, is calculated from the equation of a state for an ideal gas. The source terms, $S_i$, due to interactions between gaseous and disperse phases are expressed using the total number of particles, $N$, existing in the control volume of the gaseous phase calculation:

$$S_m = -\frac{1}{\Delta V}\sum_N \dot{m}_p, \tag{5}$$

$$S_{ui} = -\frac{1}{\Delta V}\sum_N \left[\frac{m_p f_1}{\tau_p}(u_i - u_{p,i}) + \dot{m}_p u_{p,i}\right], \tag{6}$$

$$S_h = -\frac{1}{\Delta V}\sum_N \left[\frac{1}{2}(m_p u_{p,i} u_{p,i}) + Q_p + \dot{m}_p h_{V,S}\right], \tag{7}$$

$$S_{Y_k} = -\frac{1}{\Delta V}\sum_N \dot{m}_p, \quad \text{for fuel} \tag{8}$$

$$S_{Y_k} = 0, \quad \text{for other chemical species} \tag{9}$$

where $m_p$ and $\dot{m}_p$ are the particle mass and $dm_p/dt$, respectively, $u_{p,i}$ is the particle velocity, $\Delta V$ is the volume of the control volume for the gaseous phase calculation, and $h_{V,S}$ is the evaporated vapor enthalpy at the particle surface. $Q_p$ is the convective heat transfer.

The liquid particles are tracked individually in a Lagrangian manner using equations (10) and (11).

$$\frac{dx_{p,i}}{dt} = u_{p,i}, \tag{10}$$

$$\frac{du_{p,i}}{dt} = \frac{f_1}{\tau_p}\left(u_i - u_{p,i}\right). \tag{11}$$

Here, $x_{p,i}$ is the particle position. Time variation of particles temperature, $T_p$, is considered as sum of the convective heat transfer and the latent heat of vaporization but it is skipped here. The particle response time $\tau_p$ is defined by

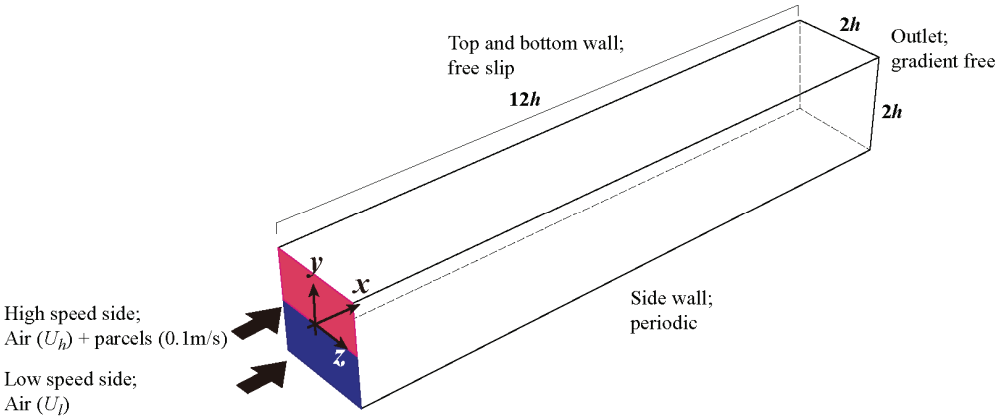


**Figure 1** Schematic of calculation grid for mixing layer.

$$\tau_p = \frac{\rho_p/\rho D_p^2}{18\nu}, \tag{12}$$

where $D_p$ is the particle diameter and $\nu$ is dynamic viscosity. $\rho_p$ is particle material density. Concerning the vaporization of particles, a nonequilibrium Langmuir-Knudsen evaporation model is chosen[7]. $f_1$ is the correction coefficient of Stokes drag for evaporation particle[8].

$$f_1 = \frac{1 + 0.0545\mathrm{Re}_{sl} + 0.1\mathrm{Re}_{sl}^{1/2}(1 - 0.03\mathrm{Re}_{sl})}{1 + b|\mathrm{Re}_b|^c}, \tag{13}$$

$$b = 0.06 + 0.077\exp(-0.4\mathrm{Re}_{sl}), \tag{14}$$

$$c = 0.4 + 0.77\exp(-0.04\mathrm{Re}_{sl}). \tag{15}$$

Where the particle Reynolds number based on the slip velocity, $U_{sl}=|u_i-u_{p,i}|$, and Reynolds number based on the blowing velocity $U_b$ are defined as

$$\mathrm{Re}_{sl} = \frac{U_{sl}D_p}{\nu}, \tag{16}$$

$$\mathrm{Re}_b = \frac{U_bD_p}{\nu}. \tag{17}$$

It is assumed that $\rho_p$ is much larger than $\rho$ such that the dominating forces acting on the particle by the surrounding fluid are the drag and lift, and other forces (the pressure gradient, added mass, and Basset) are neglected.

In this study, n-decane ($\rho_p$ = 642kg/m$^3$) is used as injected particles. Particle volume fraction is $2.0\times10^{-5}$ at the inlet of the high-speed side of the mixing layer. The initial particle size distribution is obtained by approximating the past Phase Doppler Anemometry (PDA) measurement[9] of sprayed n-decane fuel with Nukiyama-Tanasawa equations[10]. Sauter mean diameter (SMD) is 74.2μm. Effects of a parcel modeling on momentum transfer between two-phases, change of flow field and scalar transfer by evaporation are investigated. As parcel modeling, 10 particles are represented by one parcel in NFM and around 10 particles are represented by one parcel in VFM. Total parcel numbers in VFM and NFM are approximately the same. And they are compared to RC in which one parcel represents one particle.

***Computational details***

Figure 1 shows the schematic of the computational domain. The three-dimensional domain is 600 mm (12$h$), 100 mm (2$h$) and 100 mm (2$h$) in the streamwise ($x$), transverse ($y$) and spanwise ($z$) directions. The numbers of the non-equally distributed grid points used here are 388 × 128 × 128 in streamwise, transverse and spanwise directions. The origin of the coordinate axes is set at the center of the inlet boundary. Droplet parcels are injected uniformly into the high-speed side of the mixing layer with initial streamwise velocity, 0.1 m/s. The high- and low-speed free-stream velocities are $U_h$ = 3.8 m/s and $U_l$ = 0.98 m/s, respectively. The vertical distributions of the time averaged velocity and fluctuation velocity are given by the DNS data of Kim *et al.*[11] Turbulent Reynolds numbers are 180 and 590 for low- and high-speed side. It should be noted that the cases of initial turbulent intensity at low speed side and particle SMD which can be characterized as the moderate Stokes number (St~1)

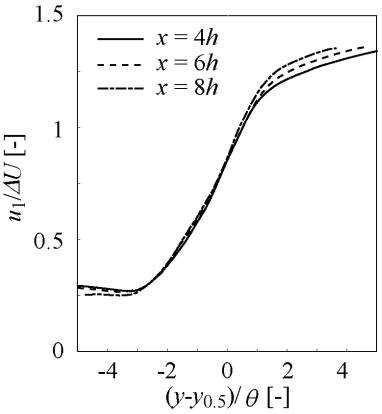


**Figure 2** Time-averaged mean velocity in the mid-*z* plane.

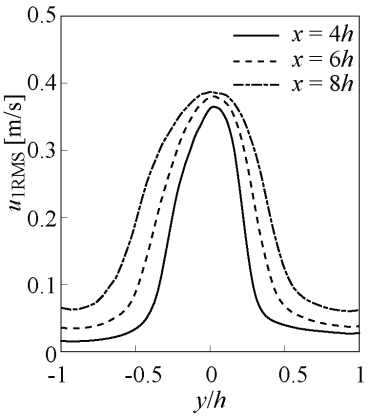


**Figure 3** Streamwise RMS velocity without particles in the mid-*z* plane.

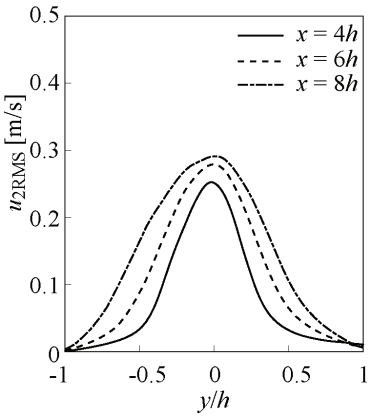


**Figure 4** Transverse RMS velocity without particles in the mid-*z* plane.

are examined in this study. The gradient-free condition for the pressure and velocity is applied to the domain outlet. Slip boundary conditions are imposed on the velocity components on the top and bottom walls.

**Results and Discussion**

***Flow properties without particles***

Figure 2 is the non-dimensional time-averaged velocity on three cross-stream sections. The transverse distance, $y$, is normalized by using the momentum thickness $\theta$, and $y_{0.5}$, which is the transverse location of $u_1$-$U_l/\Delta U$=0.5 to verify the trend of mean velocity profile where $\Delta U = U_h - U_l$. $\theta$ is calculated using equation (9). Over line in the equation means time averaging. The non-dimensional velocities on three cross-stream sections distribute almost on one curve, suggesting that a fully developed mixing layer is calculated from $x$=4$h$ to 8$h$. Some deviation at $(y-y_{0.5})/\theta$ <-4 or $(y-y_{0.5})/\theta$ >2 exists owing to a shortage of transverse length in the flow field in this study.

$$\theta = \frac{1}{\Delta U^2} \int_{-0.5}^{+0.5} (U_h - \overline{u_1})(\overline{u_1} - U_l)\, dy. \tag{18}$$

Figures 3 and 4 are the RMS value of fluctuation velocity on three cross-stream sections in mid-$z$ plane. It is observed the fluctuation generated near $y/h$=0 diffuses to top and bottom walls as $x$ increases. A trend of an increase of RMS velocity at the center ($y/h$=0) in transverse direction agrees with previous study[3].

***An effect of parcel models on particles dispersion from upper side to bottom side of the mixing layer***

Figures 5 to 13 show probability density function of the number of particles distributed in bottom side of the mixing layer at 4$h$, 6$h$ and 8$h$ in streamwise direction. Particles are sampled from a cubic are of $x$=3$h$ to 5$h$, $y$=-1$h$ to 0, $z$=-1$h$ to 1$h$ for at $x$=4$h$, $x$=5$h$ to 7$h$ for 6$h$ (for $y$, $z$ direction, the same as at $x$=4$h$), $x$=7$h$ to 9$h$ for 8$h$. The number of particle is counted based on each parcel models and are sorted by diameter and the sum of all distributions is unity in each figures. At $x$=4$h$, particles whose diameter is 41-60μm are most transferred particles from upper side in RC. Distributions of 21-40μm is the second and 61-80μm is the third. This is considered to be that the particles whose diameter is less than SMD (74.2μm in this study) and Stokes number is small (St<1), are more likely to be transferred by vorticity motion. NFM (figure 11) reproduces this trend of RC well compared to VFM (figure 8). The trend of distributions in NFM at $x$=6$h$ (figure 12) also shows good agreement with that of RC (figure 6) compared to that of VFM (figure 9). Fluctuation of distribution along with $y/h$ in the case of VFM (figure 9) is due to that the small number of parcels including a number of small diameter particles which distribute discretely in space. At $x$=8$h$, the trend of distributions in VFM fluctuates along with $y/h$ as much as NFM. This is due to discrete distribution of parcels in space.

***An effect of parcel models on momentum transfer between two-phases and flow properties***

Figure 14 shows instantaneous particles distribution with isosurface of vorticity distribution. Red dots represent spatial position of particles. As vorticity develops downstream, particles get involved and transferred to the lower side of flow field.

Figures 15 to 17 show time-averaged momentum transfer between two-phases at each streamwise position in

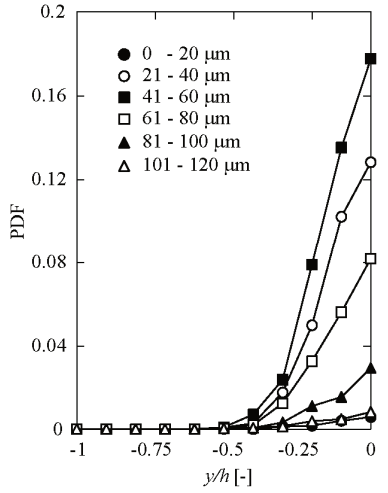


**Figure 5** Time averaged particle diameter distribution in RC at 4*h*.

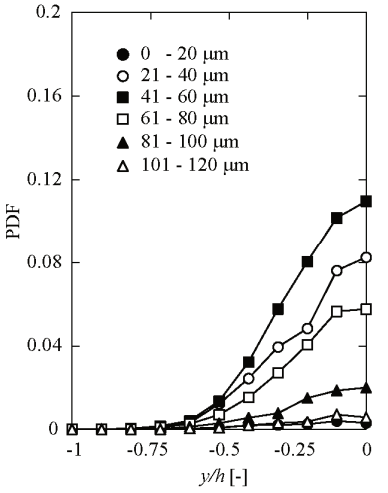


**Figure 6** Time averaged particle diameter distribution in RC at 6*h*.

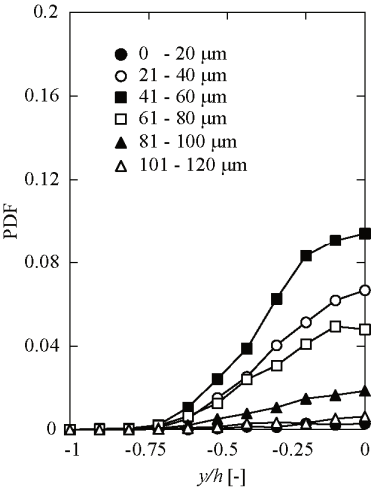


**Figure 7** Time averaged particle diameter distribution in RC at 8*h*.

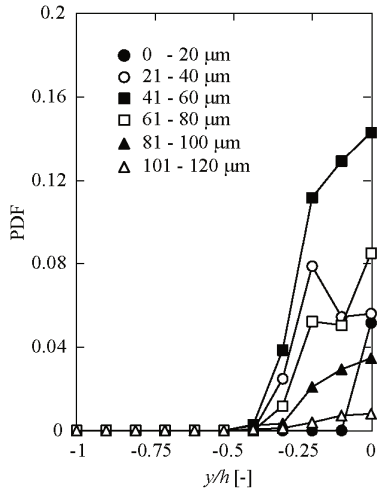


**Figure 8** Time averaged particle diameter distribution in VFM at 4*h*.

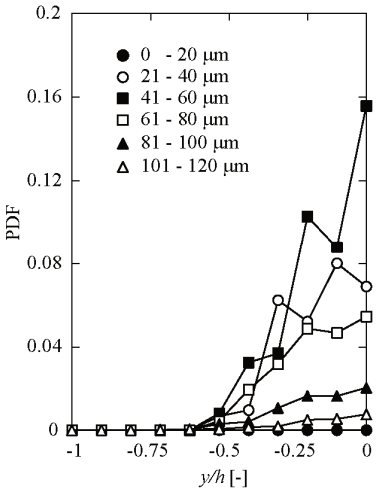


**Figure 9** Time averaged particle diameter distribution in VFM at 6*h*.

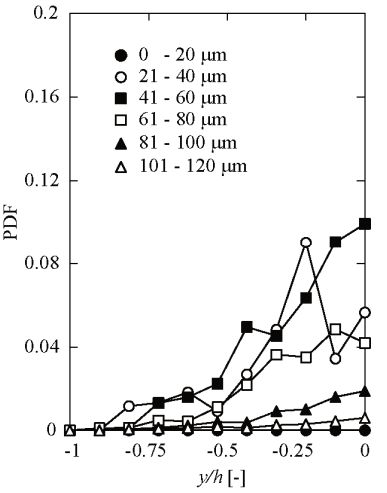


**Figure 10** Time averaged particle diameter distribution in VFM at 8*h*.

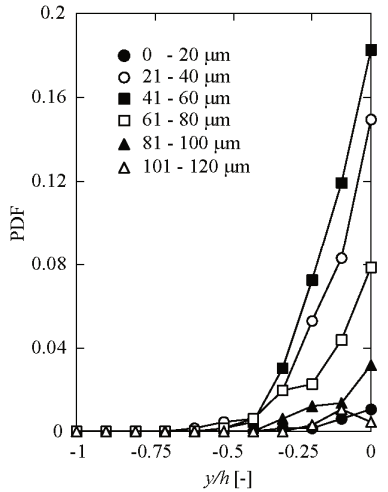


**Figure 11** Time averaged particle diameter distribution in NFM at 4*h*.

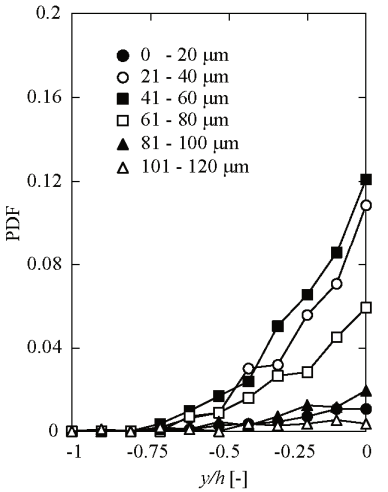


**Figure 12** Time averaged particle diameter distribution in NFM at 6*h*.

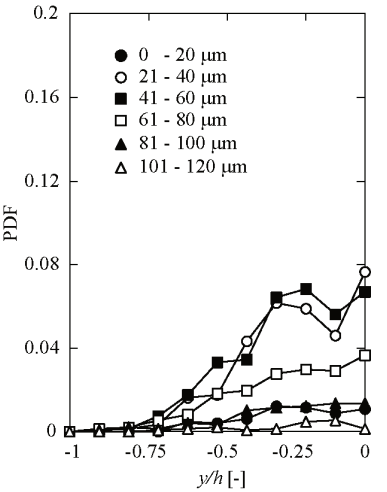


**Figure 13** Time averaged particle diameter distribution in NFM at 8*h*.

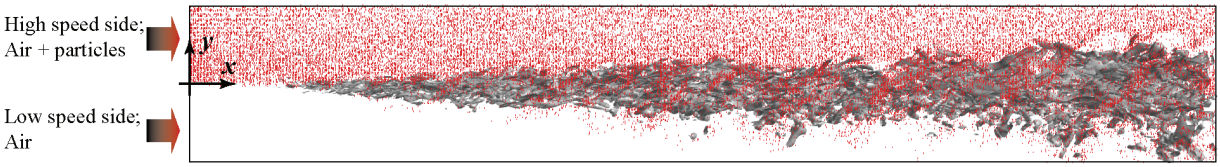


**Figure 14** Instantaneous isosurface of vorticity (gray cloud) and particle distribution (red dots) when no parcel model is applied.

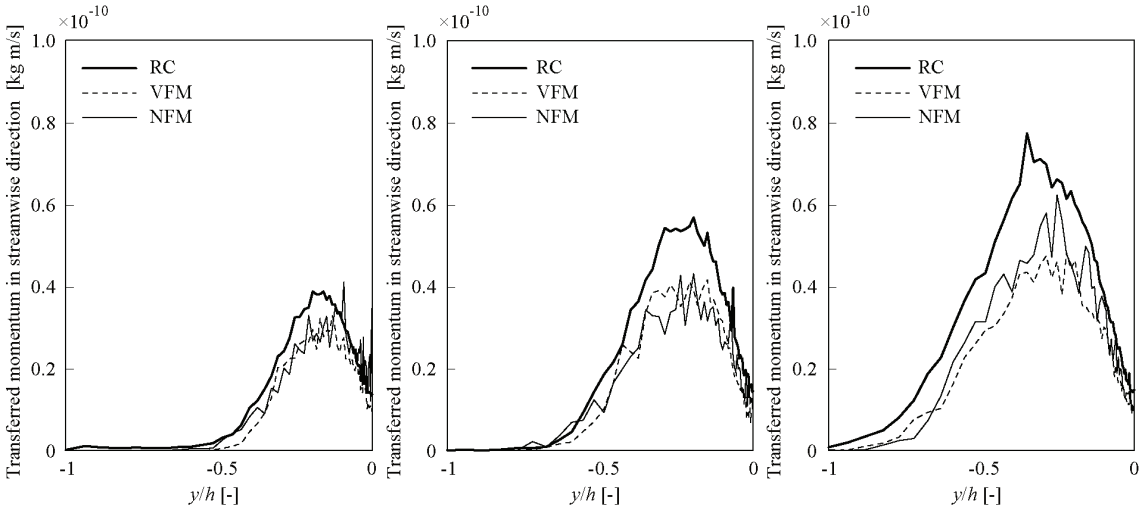


**Figure 15** Time averaged absolute transferred momentum between two-phases at 4*h*.

**Figure 16** Time averaged absolute transferred momentum between two-phases at 6*h*.

**Figure 17** Time averaged absolute transferred momentum between two-phases at 8*h*.

mid-*z* plane. In this study, the amount is calculated using absolute value of momentum in each time step. Hence the sign of obtained averaged momentum is indistinctive. Each figure indicates spatial distribution of momentum transportability. For all positions, distribution of without parcel model is relatively smooth because the total number of particles (that is corresponding to the total number of parcels in RC) distributed in space is larger than other cases using parcel model. Peaks found around $y/h$=-0.2 at $x$=4$h$, $y/h$=-0.25 at $x$=6$h$ and $y/h$=-0.3 at $x$=8$h$ indicates that the relative velocity between outer edge of vorticity structure and parcels is large in this region. At $x$=4$h$ and 6$h$, both parcel models underestimate momentum transfer between -0.4<$y/h$<-0.1. This is because the parcels exchange a large amount of momentum in the limited small spaces. This decreases the relative velocity at limited locations, and suppresses the total momentum exchange.
Relatively large discrepancy found around $y/h$<-0.4 at $x$=8$h$ between RC and VFM or NFM compared to $x$=4$h$ and 6$h$ comes from the momentum, which is generated around $y/h$~0.25, transferred by vorticity motion.

Figures 18 to 20 show root mean square value of the fluctuation velocity in streamwise direction at each streamwise position. Basically, fluctuation in the flow field is increased by particles not depending on the parcel models. The largest difference between the case without particle and the case with particles found around $y/h$~-0.2 at $x$=0.4$h$, $y/h$~-0.4 at $x$=0.6$h$, $y/h$~-0.6 at $x$=0.8$h$. This shift of the largest difference is corresponding to the shift of the peak of momentum transfer found in figures 15 to 17 and it is deduced that momentum is mainly transferred from effective particles whose Stokes number is over unity to ambient fluid and then diffuses from the center region to bottom region of the mixing layer. However, it is considered that transferred momentum is not so large that a difference between parcel models doesn't appear clearly. Deviation of RC from two parcel models near the bottom wall of mixing layer around $y/h$~-0.9 seen in figures 19 and 20 is due to that the number of particles transported with parcel model is small compared to the case of RC. A critical number at which turbulent state changes significantly compared to RC needs further investigation.

***An effect of parcel models on a vaporised scalar diffusion yield from dispersed particles***

Figures 21 to 23 are the scalar fraction of evaporated n-decane yield from particles. Evaporation occurs most along the center line ($y/h$=0) of the mixing layer in all cross-stream sections and vapor diffuses from the center line to the bottom wall as increase of $x$. Basically, reproducibility of the NFM is better than VFM compared to RC along transverse direction or all cross-stream sections. The reason of that is considered to be as follows: in

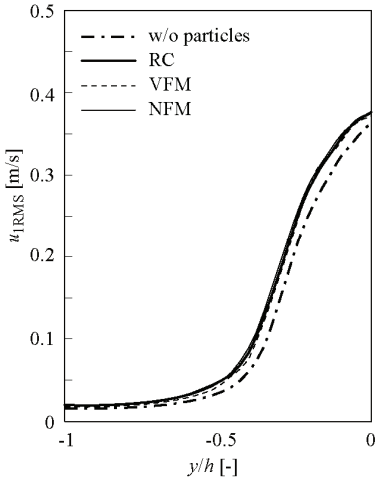


**Figure 18** Streamwise RMS velocity with particles at 4*h*.

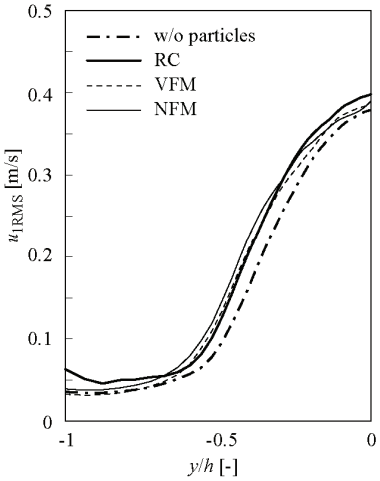


**Figure 19** Streamwise RMS velocity with particles at 6*h*.

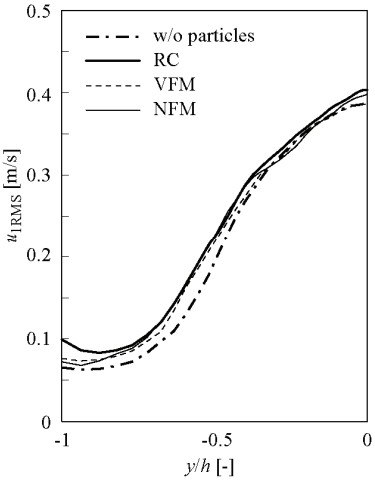


**Figure 20** Streamwise RMS velocity with particles at 8*h*.

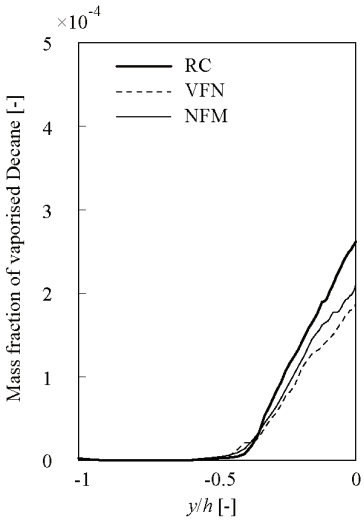


**Figure 21** Spatial fraction of evaporated n-decane at 4*h*.

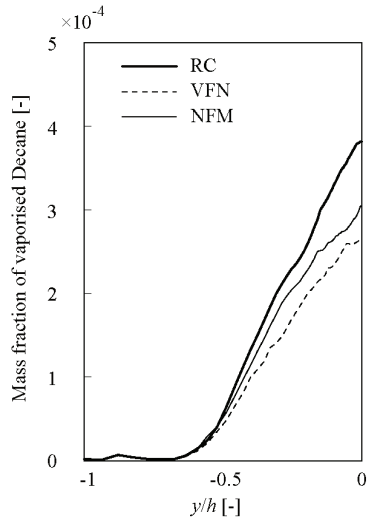


**Figure 22** Spatial fraction of evaporated n-decane at 6*h*.

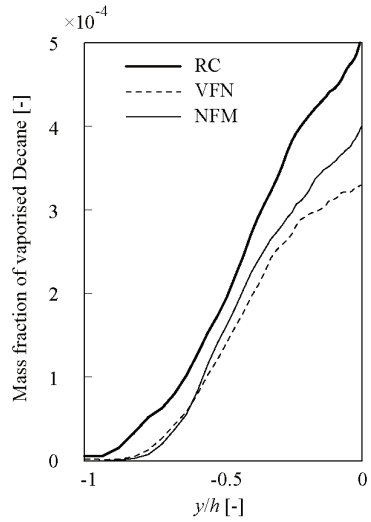


**Figure 23** Spatial fraction of evaporated n-decane at 8*h*.

the evaporation model adopted in this study, evaporation rate becomes large as droplet diameter becomes small, while evaporation rate is reduced as scalar fraction of n-decane becomes high. Hence, the evaporation rate of the parcel which represents a number of small particles becomes small rapidly in the VFM. Subsequently, total amount of evaporation is underestimated by the VFM compared to NFM and RC.

In this study, an effect of parcel models on the change of turbulent flow field is not significant as described in previous section. However, when an effect of parcel models on ambient flow field becomes significant, evaporation rate will also be affected indirectly by a change of scalar fraction around particles and diffusion of vapor will be also affected.

**Summary and Conclusions**

A direct numerical simulation was applied to a particle laden mixing layer, and effects of a difference of parcel models (VFM, NFM) on the dispersion of particles, the momentum transfer between two-phases, flow field and scalar diffusion were investigated. The main results from this study can be summarized as follows.

For dispersion of particles, it is found in comparing with RC that the spatially fluctuated distribution of particles and low dispersivity appear for VFM, while it shows a good agreement for NFM. This is because a number of small particles are represented by one parcel in VFM and it disperses locally.

For momentum transfer between two-phases, parcel models trace the tendency of the transfer in RC. However, both models underestimate quantitatively. This is considered due to that the parcels exchange a large

amount of momentum in the limited small spaces compared to RC. This decreases the relative velocity at limited locations, and suppresses the total momentum exchange.

For turbulent flow field, there is no significant difference among the parcel models and RC. The reason is considered due to that the turbulent intensity of the original flow field adopted in this study is so large that an effect of particles can be neglected.

For diffusion of scalar evaporated from particles, the parcel models trace the spatial tendency of the change of scalar compared to RC. However, both models underestimate the total amount of evaporation because the increase of mass fraction is localized by the parcel modeling and the evaporation rate is suppressed by the increase of mass. Especially, VFM in which one parcel representing many small particles is more likely to underestimate the total amount of evaporation compared to NFM.

**References**

[1] Yang, Y., Chung, J.N., Troutt, T.R., Crowe, C.T., *Physics of Fluids* A-2: 1839–1845 (1990).
[2] Dimas, A.A., Kiger, K.T., *Physics of Fluids* 10: 2539–2557 (1998).
[3] Michioka, T., Kurose, R., Sada, K. and Makino, H., *International Journal of Multiphase Flow*, 31: 843–866 (2005).
[4] Moriai, H., Kurose, R., Watanabe, H., Tano, Y., Akamatsu, F. and Komori, S., Submitted to *Fuel* (2012)
[5] Arai, J., Oshima, N., Oshima, M., Ito, H. and Kubota, M., *Journal of Fluid Science and Technology* 2-3: 601-610 (2007).
[6] Nakamura, M., Akamatsu, F., Kurose, R. and Katsuki, M., *JSME International Journal Series B* 49-2: 498-505 (2006).
[7] Miller, R. S., Harstad, K. and Bellan, J., *International Journal of Multiphase Flow* 24: 1025-1055 (1998).
[8] Kurose, R., Makino, H., Komori, S., Nakamura, M., Akamatsu, F. and Katsuki, M., *Physics of Fluids* 15: 2338-2351 (2003).
[9] Watanabe, H., Kurose, R., Hwang, SM. and Akamatsu, F., *Combustion and Flame* 148: 234-248 (2007).
[10] Nukiyama, S. and Tanasawa, Y., *Transactions of the Society of Mechanical Engineers Japan* 5-18: 62-67 (1939). *in Japanese*
[11] Kim, J., Moin, P. and Moser, R., *Journal of Fluid Mechanics* 177: 133-166 (1987).